



Analysis of Gaseous Hydrogen Refueling Process to Develop Thermodynamic Model

Byung Heung Park¹

Received: 8 February 2024 / Revised: 24 March 2024 / Accepted: 26 March 2024 / Published online: 2 April 2024
© The Author(s), under exclusive licence to Korean Institute of Chemical Engineers, Seoul, Korea 2024

Abstract

Hydrogen is an energy source that is expected to play a major role in energy transition policies that replace fossil fuels. Currently, the main demand for hydrogen is the transportation sector. As the number of fuel cell electric vehicles increases, it has become essential to develop a hydrogen refueling protocol which is a method of safely filling hydrogen associated with hydrogen refueling stations. Hydrogen refueling protocols are proposed to be developed based on thermodynamic models and verified through experimental studies. Developing a simulation model requires thermodynamic analysis of the hydrogen filling process, but such research has not been conducted. In this study, thermodynamic phenomena are analyzed, which take place during the high-pressure hydrogen refueling process using a generic correlation equation with different coefficients corresponding to various thermodynamic properties. By quantitatively analyzing the Joule-Thompson effect which occurs when hydrogen is supplied to an on-board tank, the degree of temperature rise is estimated depending on the hydrogen refueling station operation method. The quantitative contribution of kinetic energy is also analyzed. The kinetic energy is often ignored in a governing equation of thermodynamic models expressed as an energy balance but it is revealed that the term cannot be ignored in high-flow filling process. Inaccuracy which arises when stagnation enthalpy is used instead of static enthalpy in a thermodynamic model is also reviewed, providing a basis for developing a new thermodynamic model.

Keywords Hydrogen refueling process · Thermodynamic model · Joule–Thompson effect · Kinetic energy contribution · Stagnation enthalpy

Introduction

The world has utilized a diverse range of energy sources that can be either directly harvested from nature (primary energy) or produced by conversion of primary energy resources (secondary energy). Currently, fossil fuels such as coal, petroleum, and natural gas are the dominant primary energy sources in the world. However, the fossil fuels are finite resources and their supply is inevitably limited [1]. Therefore, it is quite difficult to sustainably continue to use the fossil fuels while maintaining or increasing the current energy consumption rate. Moreover, the use of the fossil fuels can have a negative impact on the environment because the burning of the fossil fuels releases greenhouse

gases into the atmosphere, which trap heat and cause global warming. As the dependence on fossil fuels decreases due to their decreasing availability and increasing environmental concerns, the world will become more reliant on alternative energy sources.

Hydrogen is a promising energy carrier with more sustainable feature than traditional energy sources because it has the potential to be produced, stored, and transported in a clean and efficient way. It can be directly used as a fuel for gas turbine power plants or converted into electricity by well-established devices such as fuel cells. One of the main reasons why hydrogen is attracting attention is that it is a complementary energy carrier for electricity. Hydrogen can be used to balance a power grid and provide flexibility when there is excess or insufficient electricity generation. The concept of a hydrogen economy where hydrogen and electricity are used as complementary secondary energy carriers has been contemplated for many decades [2–5].

Recently, the policy of energy transition becomes critical issue around the globe [6, 7]. The main drivers of the policy

✉ Byung Heung Park
b.h.park@ut.ac.kr

¹ Department of Chemical and Biological Engineering,
Korea National University of Transportation, 50 Daehak-ro,
Chungju-si, Chungcheongbuk-do 27469, Republic of Korea

are the need to reduce the emission of the greenhouse gases and the increasing cost of the fossil fuels. Hydrogen technology with sustainability and environmental friendliness has been recognized to be the most promising choice for realizing the energy transition [8]. One of the key elements of energy transition is to electrify transportation which means switching from gasoline and diesel vehicles to battery and fuel cell electric vehicles (FCEVs) [9, 10].

Transport is acknowledged as a challenging sector to decarbonize because the transportation sector mostly depends on the fossil fuels for its service and accounts for 17% of global CO₂ emissions by using about 18% of primary energy consumption [11]. Therefore, FCEV is recognized as one of the most important technologies to accomplish decarbonization in the transport sector under the energy transition policy [12, 13]. FCEVs generally present better fuel economy than internal combustion engine vehicles (ICEVs) burning gasoline or diesel. Light FCEVs can provide a driving range of up to 500 km consuming about 5 kg of hydrogen [14]. In addition, hydrogen can be readily refueled into FCEVs as quickly as gasoline or diesel into ICEVs. The advantages of using hydrogen and FCEVs make it particularly suitable for replacing ICEVs in long distance driving or heavy weight delivering [15, 16].

Republic of Korea (ROK) is one of the leading countries in hydrogen. The government of ROK decided to investigate hydrogen industry and announced its own Hydrogen Economy Roadmap in 2019 addressing its targets to 2040 [17]. The plan was promoted with the aim of improving energy security by reducing the amount of energy imported from foreign countries under economic and environmental considerations. The action plans of the roadmap primarily concern the transportation section mainly focused on FCEVs and hydrogen refueling infrastructures [18, 19]. ROK plans to increase FCEVs production to 100,000 units by 2025, with 40,000 units for export. The roadmap also contains the strategy for expanding domestic hydrogen refueling stations (HRSs) up to 1200 by 2040 [17].

The main purpose of HRSs is to refuel FCEVs safely and rapidly [20]. The performance of HRSs is governed by hydrogen refueling protocol which is temporal procedures that control the filling rate [21]. Currently, most of FCEVs store hydrogen in the form of highly compressed gas. The hydrogen filling rate must be controlled for safe use of the hydrogen storage tank since the process of compressing the gaseous hydrogen at high pressure is accompanied by an increase in temperature. SAE (Society of Automotive Engineers) J2601 is recognized as an international standard protocol for light duty vehicles [22]. However, the application of the protocol is limited by a mass flow rate, a tank storage capacity, a precooling capability, and so on. Therefore, innovative hydrogen refueling protocol has been developed

and proposed to improve the utilization of HRSs based on thermodynamic models [23, 24].

Hydrogen refueling protocols should provide guidelines for a hydrogen filling process in various situations. The temperature rise which occurs during the process of hydrogen refueling depends on the type of storage tank, the mass flow rate, the ambient temperature, and the initial pressure and temperature of hydrogen in on-board tank, the temperature of the hydrogen dispensed from HRS, and the ambient temperature. Therefore, hydrogen refueling protocols are developed based on thermodynamic models which can reflect these sophisticated phenomena.

Apart from the development of hydrogen refueling protocols, thermodynamic models have been also used to analyze and predict temperature and pressure changes of hydrogen in on-board tanks during rapid filling process. The efforts for analyzing thermodynamics of refueling to FCEVs have been focused on light-duty vehicles of which storage capacity are usually less than 10 kg of hydrogen [25, 26]. A simple thermodynamic model for refueling FCEV with capacity of 7 kg hydrogen was developed by Rothuizen et al. [27] by ignoring the thermal mass between HRS and vehicle on-board tank.

Recently, 3D computational fluid dynamic (CFD) models [28–31] have been examined and the temperature distribution inside the on-board tank has been assessed with respect to the filling conditions. Highly advanced computational methods such as machine learning [32] and artificial neural networks [33] have also been applied to hydrogen refueling models for predicting the temperature and the pressure of hydrogen. However, thermodynamic models which associated with fluid dynamics and thermal interactions are still being developed on a theoretical basis that reflects physical phenomena and used as a method to simulate hydrogen refueling process [34–37].

Most of thermodynamic models [38–41] have been proposed by coupling an energy balance for gas inside on-board tank with heat transfer equations through the wall of the tank. The thermodynamic behavior of hydrogen occurring during the filling process is related to the energy balance equation. In practice, the approach to developing a thermodynamic model is to establish a generalized energy balance equation and then simplify the equation by reflecting the filling process and characteristics of hydrogen. Therefore, it is necessary to analyze the thermodynamic behavior of hydrogen and simplify the equation accordingly.

In this context, the present work addresses comprehensive analysis on thermodynamic properties of hydrogen for the development of zero-dimensional (lumped parameter) thermodynamic models describing a refueling process. The essence is to provide the theoretical background for understanding the process and to determine the conditions under which assumptions can be applied.

The Joule–Thomson (JT) effect, which can explain temperature changes due to pressure drop during the refueling process, is quantitatively analyzed with options of a hydrogen refueling station. Then, the influence of kinetic energy, which is ignored in most thermodynamic models [42–44] but some authors [45–47] included the term in an energy balance, is analyzed and it was shown that the contribution of kinetic energy cannot be ignored under high flow conditions. The difference in temperature rises that occur when stagnation enthalpy rather than static enthalpy is used in thermodynamic models is also studied with various mass flow rate.

Hydrogen Refueling Process and Hydrogen Properties

Currently, most of commercial FCEVs adopt a compressed hydrogen storage system (CHSS) composed of on-board tanks, pressure relief devices and shut off devices. During refueling, hydrogen flows from a high-pressure tank at a HRS into the vehicle tank only based on pressure difference. A typical connection for filling hydrogen is represented in Fig. 1. Schematically, a representative HRS consists of a hydrogen storage system, a pressure reduction valve, and a pre-cooler [48, 49]. The hydrogen storage system can be set up by two types: (a) buffer system or (b) cascade system [50–52]. In general, three storage tanks at different pressure level are used in the cascade system while a single tank at high pressure is required in the buffer system.

The desired pressure and temperature of the dispensed hydrogen are controlled by the pressure reduction valve and the pre-cooler, respectively. The hydrogen is cooled down before being introduced into a vehicle to prevent the on-board tanks from overheating beyond a safety limit temperature.

Hydrogen which has been stagnant in the storage tank of a HRS flows and undergoes temperature and pressure changes during the refueling process and is ultimately stored in a stagnant state in the on-board tanks of a vehicle. The thermo-physical properties of hydrogen must be accurately estimated to analyze the thermodynamic phenomena taken place during the process. Recently, a universal equation in a polynomial form has been proposed with coefficients determined by a machine learning method [53] using reference data from NIST (National Institute of Standards and Technology) Chemistry Webbook [54]. Various hydrogen properties such as density, internal energy, enthalpy were accurately reproduced within the temperature and pressure range targeted for simulations of the refueling process. The average and maximum relative error deviated from the reference data are below 0.3% and 2.5%, respectively, for thermo-physical properties except for entropy.

The following polynomial equation is applied to correlate property Y with two different thermodynamic properties of X_1 and X_2 [53].

$$Y = \sum_{i=0}^N \sum_{j=0}^{N-i} a_{ij} X_1^i X_2^j \tag{1}$$

where N is the order of the polynomial Eqs. (2–5) and a_{ij} is a coefficient of the product of the i^{th} power of X_1 and the

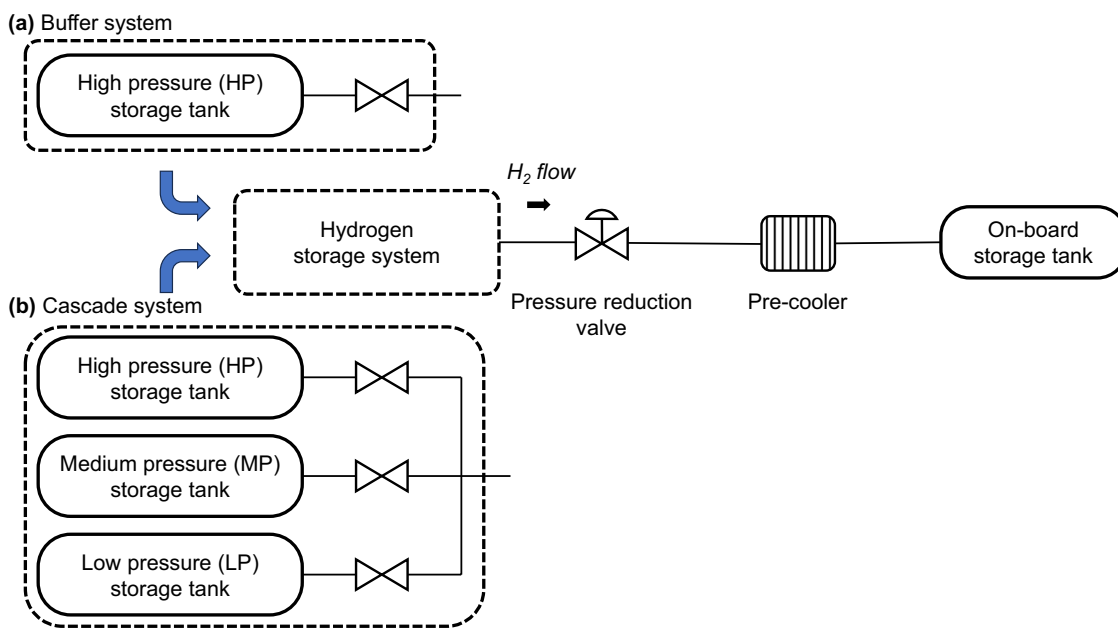


Fig. 1 Schematic description of typical connection for hydrogen filling into FCEV: **a** buffer system and **b** cascade system

j^{th} power of X_2 . In this work, the 5th order equation ($N=5$) is used to correlate the thermodynamic property of Y with respect to temperature $T (=X_1)$ and pressure $P (=X_2)$. Different values of a_{ij} are used depending on the thermodynamic property to be estimated, and the values of the coefficients are summarized in Table 1.

Process Analysis from Thermodynamic Perspective and Discussion

Energy Balance

The main purpose of developing a thermodynamic model for the hydrogen refueling process is to predict the temperature and pressure changes in the on-board tank during the filling process. The temperature as well as the pressure increases due to the accumulation of mass and energy accompanied by a hydrogen inflow.

Usually, a hydrogen storage tank has only one inlet and, thus, a material balance is relatively simple, but an energy balance is expressed somewhat complexly because there are many things to consider. The energy balance for the on-board tank with a single inlet is expressed as Eq. (2) which neglects a viscous work associated with a fluid flow.

$$\frac{dU}{dt} = \frac{d(mu)}{dt} = \dot{Q} + \dot{m}_{\text{in}} \left(h_{\text{in}} + \frac{v_{\text{in}}^2}{2} + gz_{\text{in}} \right) \quad (2)$$

The energy of the hydrogen is accumulated in the form of the total internal energy $U (=mu)$ because the hydrogen is stored in a stagnant state. Enthalpy h , kinetic energy $v^2/2$, and potential energy gz are associated with specific energy of the hydrogen inflow. The heat-rate term \dot{Q} is also included to consider a thermal interaction of the hydrogen stored tank with the environment.

Joule–Thomson (JT) Effect

The Joule–Thomson (JT) effect describes the temperature change of a real gas when it is forced to flow through a valve or a porous plug without exchanging heat with the environment. The pressure of the fluid is decreased passing through the valve or the porous plug under the isenthalpic process while maintaining kinetic energy. Therefore, a Joule–Thomson (JT) coefficient defined as the isenthalpic change in temperature of the fluid due to pressure drop is given as

$$\mu_{\text{JT}} = \left(\frac{\partial T}{\partial P} \right)_H \quad (3)$$

Table 1 Coefficients of Eq. (1) for property Y with T [K] and P [MPa]

	Thermodynamic property (Y)				
	JT coefficient (μ_{JT}) [K/MPa]	Enthalpy (h) [kJ/mol]	Internal Energy (u) [kJ/mol]	Density (ρ) [mol/L]	Heat capacity (c_p) [J/mol K]
a_{00}	2.14875E+00	4.66229E-01	6.33535E-01	1.22604E+01	1.66606E+01
a_{10}	-2.02751E-02	1.64538E-02	6.17436E-03	-1.79281E-01	9.08579E-02
a_{20}	6.68982E-05	5.33749E-05	6.19640E-05	1.02937E-03	-2.18894E-04
a_{30}	-1.14061E-07	-1.18416E-07	-1.35044E-07	-2.90490E-06	1.43492E-07
a_{40}	9.37501E-11	1.42185E-10	1.54270E-10	4.03358E-09	1.33298E-10
a_{50}	-2.71780E-14	-7.46273E-14	-7.47212E-14	-2.20656E-12	-1.36154E-13
a_{01}	-9.63684E-02	-2.85295E-02	-3.39284E-02	1.46962E+00	3.25658E-01
a_{11}	6.77728E-04	1.92851E-04	1.64904E-04	-6.43678E-03	-1.05279E-03
a_{21}	-1.84939E-06	-2.19611E-07	-2.87898E-07	1.18840E-05	-1.08098E-06
a_{31}	2.28067E-09	-1.34257E-10	1.39510E-10	-7.23047E-09	7.69379E-09
a_{41}	-1.03651E-12	2.98774E-13	7.52154E-14	-1.29223E-12	-7.57518E-12
a_{02}	1.08612E-03	7.17895E-04	3.94198E-04	-1.51406E-02	-7.60767E-03
a_{12}	-6.36081E-06	-3.23955E-06	-1.95020E-06	7.48869E-05	3.56741E-05
a_{22}	1.19458E-08	4.86054E-09	3.40577E-09	-1.31934E-07	-5.37843E-08
a_{32}	-7.64474E-12	-2.32038E-12	-2.02090E-12	7.68085E-11	2.28465E-11
a_{03}	-4.81116E-06	-4.73414E-06	-1.83387E-06	6.59177E-05	5.59270E-05
a_{13}	2.50159E-08	1.60010E-08	7.14328E-09	-2.62691E-07	-1.94191E-07
a_{23}	-2.36381E-11	-1.32591E-11	-6.77317E-12	2.69539E-10	1.73980E-10
a_{04}	-3.14129E-10	1.39743E-08	3.17705E-09	-9.85005E-08	-1.81582E-07
a_{14}	-3.60381E-11	-2.69393E-11	-8.86794E-12	2.54693E-10	3.14024E-10
a_{05}	4.96227E-11	-1.30451E-11	1.27513E-12	-2.37334E-11	2.37059E-10

Unlike many other real gases, hydrogen exhibits negative value of μ_{JT} at ordinary temperature and pressure because its maximum inversion temperature is as low as 200 K. Therefore, hydrogen undergoes temperature increase by JT effect during the FCEV filling process. However, the temperature increase behavior of the hydrogen in the on-board tank is not directly related with the JT effect. In general, the JT effect can be observed at a fluid flowing through a pressure changing device while keeping the kinetic energy invariant. However, in the process of filling the on-board storage tank with hydrogen, there is no flow penetrating the hydrogen storage tank and the kinetic energy is instantly changed into the internal energy because the stored hydrogen is considered as a stagnation state when the inside of the tank is defined as a control volume. As noticed by Eq. (2), the rise in temperature of the stored hydrogen occurs due to the conversion of incoming energy (including enthalpy, kinetic energy, and potential energy) into internal energy. Rather, the JT effect can be found at a pressure reduction valve (see Fig. 1) during the refueling process [55].

The JT coefficient is required to estimate the temperature rise of hydrogen passing through the pressure reducing valve. The JT coefficient is associated with an equation of state (EOS) and ideal gas heat capacity by thermodynamic relations [55]. However, the accuracy depends on the choice of EOS, and in the case of hydrogen, there is a relatively large deviations from NIST data [54] when the classical cubic EOSs are used [55]. In this work, Eq. (1) with coefficients determined by regression to NIST data is applied to calculate the temperature change.

Comparisons of the calculated JT coefficients by Eq. (1) and NIST data with temperature at different pressure

conditions are presented in Fig. 2. It has been revealed that the JT coefficients are accurately reproduced with temperature and pressure. In Fig. 2, $-\mu_{JT}$ values are indicated since the JT coefficients are negative under the hydrogen refueling conditions.

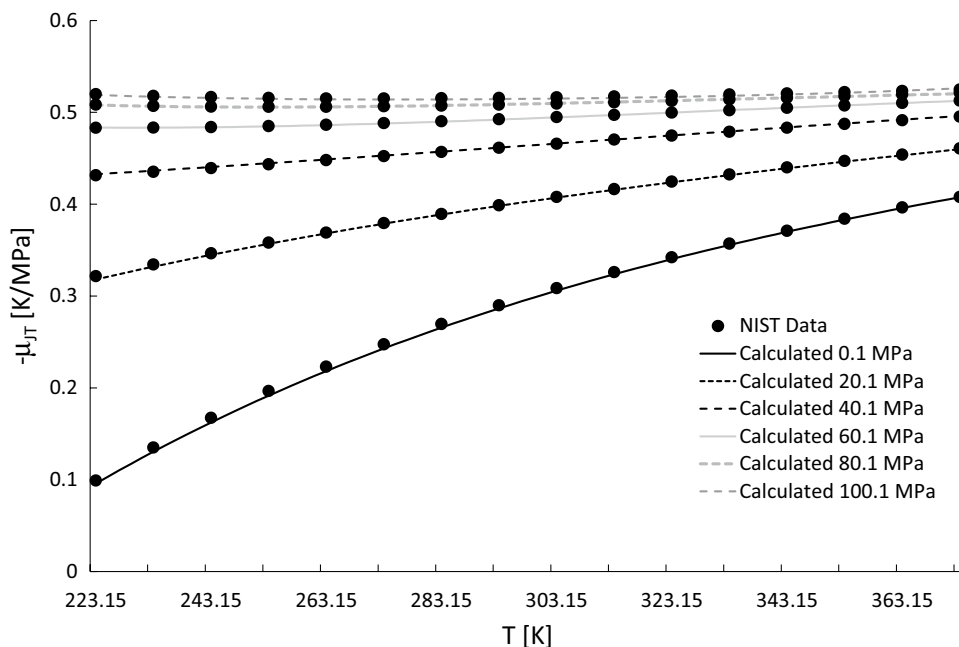
The temperature change due to the JT effect taking place at a passage of hydrogen through the pressure reduction valve is calculated by the following equation.

$$\Delta T = \int_{P_1}^{P_2} \mu_{JT} dP \tag{4}$$

Applying Eq. (1) for μ_{JT} , the temperature increase of hydrogen can be readily obtained at given upstream (P_1) and downstream pressure (P_2). The upstream pressure is the pressure of HRS storage tank, which appears as one pressure level in the buffer system and three pressures in the cascade system. As for the cascade system, the upstream pressure is shifted from a lower pressure to a higher pressure at a HRS corresponding to the downstream pressure. In order to fill hydrogen into the on-board tanks of which a nominal working pressure (NWP) is 70 MPa, the pressures of low, medium, and high pressure tank of a HRS are 25 to 50 MPa, 50 to 70 MPa, and over 90 MPa, respectively [56]. The downstream pressure is a HRS dispensing pressure, which is controlled by a refueling protocol. Usually, a constant pressure increasing rate, referred to as an average pressure ramp rate (APRR), is assigned to the downstream pressure.

Under an assumption of invariant pressures at HRS tanks, an example of pressure behavior through a pressure reduction valve is presented as Fig. 3 for a case that an FCEV at

Fig. 2 Comparison of calculated JT coefficient with NIST data



initial 10 MPa is refueled for 5 min. The storage pressures for the cascade system are taken as 25, 50, and 90 MPa at low, medium, and high pressure tank, respectively. The pressure of the buffer system is treated the same as the pressure of the high pressure tank at the cascade system. The final downstream pressure is set to 80 MPa considering a finite mass flow rate filling the FCEV up to NWP.

The extent of temperature increases after a pressure reduction valve is plotted in Fig. 4. The calculation is carried out based on the pressure difference shown in Fig. 3 at 288.15 K of the upstream temperature. The temperature

increase due to the JT effect is proportional to the degree of decompression. The highest temperature rise occurs initially in the buffer system, where the temperature rise reaches approximately 37 K. In the cascade system, the highest temperature change occurred at the moment of connection to the high pressure tank, and the hydrogen temperature is predicted to rise by about 20 K. Due to the definite temperature of hydrogen fueled to FCEVs, it is predicted that a higher heat load would be required on the pre-cooler in the buffer system than the cascade system. The effect of ambient temperature has also been analyzed

Fig. 3 Illustration of upstream and downstream pressure at pressure reduction valve for buffer system and cascade system

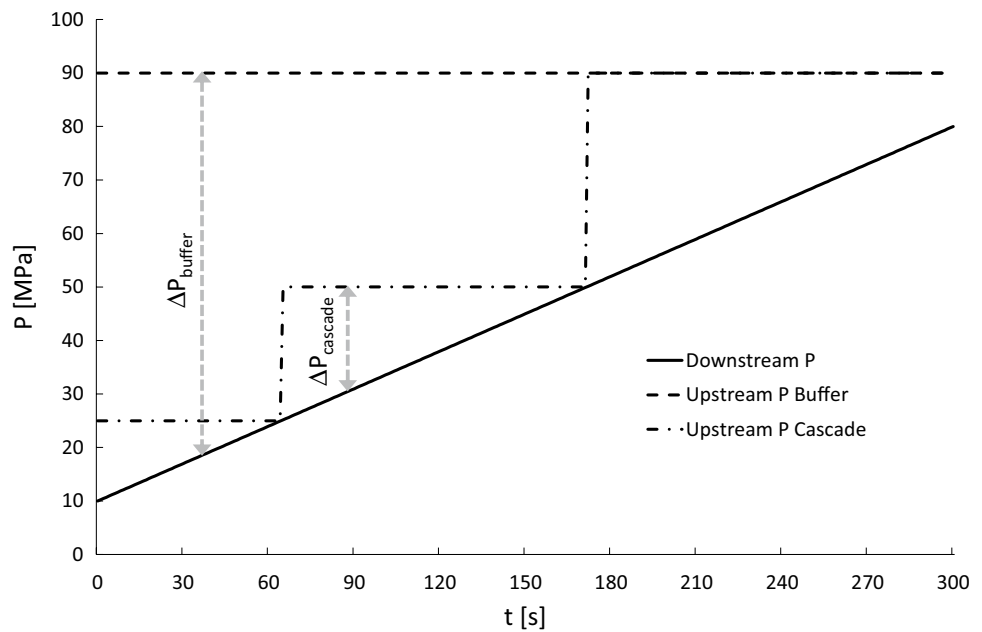
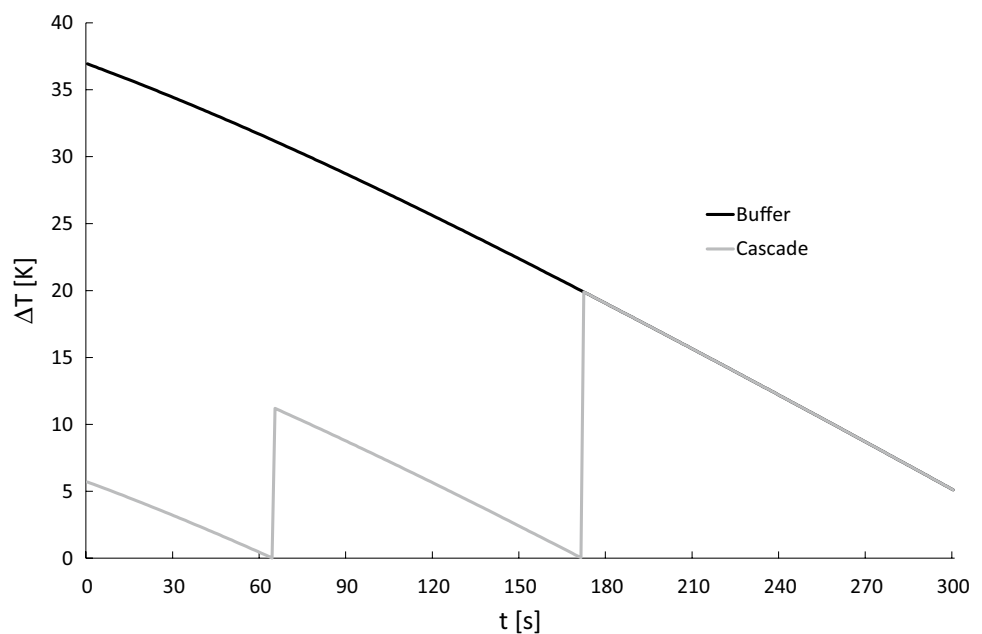


Fig. 4 Illustration of temperature increase after pressure reduction valve for buffer system and cascade system



but it is revealed that the effect is not significant on the temperature increase: the largest values are estimated as 36.2, 36.9, and 37.6 K for the buffer system at 268.15, 288.15, and 308.15 K, respectively.

Kinetic Energy Contribution

The energy flowing into an on-board storage tank includes the kinetic energy of hydrogen, as presented in Eq. (2). The flux of the kinetic energy in a thermodynamic model has been neglected in many researches [38, 42–44, 57], but some authors [39, 45–47] suggested the contribution of the kinetic energy is not negligible. Therefore, quantitative analysis of the contribution of kinetic energy on hydrogen refueling conditions is necessary for accurate thermodynamic model development.

In general, the contribution of each energy can be assessed by comparing the magnitude of enthalpy and kinetic energy in Eq. (2) since potential energy does not change in horizontal filling. Unlike kinetic energy, internal energy and enthalpy are given relative to a reference state. Therefore, Eq. (2) is expressed more precisely with the ignorance of the potential energy as follows.

$$\frac{d\{m_{\text{tank}}(u - u_0)_{\text{tank}}\}}{dt} = \dot{Q} + \dot{m}_{\text{in}} \left\{ (h - h_0)_{\text{in}} + \frac{v_{\text{in}}^2}{2} \right\} \quad (5)$$

In Eq. (5), the subscript 0 denotes a reference state. Applying the mass balance of the on-board tank ($dm_{\text{tank}}/dt = \dot{m}_{\text{in}}$), Eq. (5) can be rearranged as,

$$m_{\text{tank}} \frac{d\{(u - u_0)_{\text{tank}}\}}{dt} = \dot{Q} + \dot{m}_{\text{in}} \left\{ (h - h_0)_{\text{in}} - (u - u_0)_{\text{tank}} + \frac{v_{\text{in}}^2}{2} \right\} \quad (6)$$

Equation (6) reveals that the contribution of the kinetic energy should be analyzed by comparing with the difference of the inlet hydrogen enthalpy from the stored hydrogen internal energy. Hereinafter, the difference will be noted as e_{h-u}

$$e_{h-u} = (h - h_0)_{\text{in}} - (u - u_0)_{\text{tank}} \quad (7)$$

In Eq. (7), the enthalpy is calculated at the inflow condition while the internal energy is determined at the temperature and pressure of the hydrogen stored in a tank. NIST data presenting thermodynamic properties have been reported by adopting the normal boiling point for saturated liquid as a reference state. Therefore, the specific enthalpy and the specific internal energy values calculated by Eq. (1) imply $(h - h_0)$ and $(u - u_0)$, respectively. The calculated specific enthalpies are compared with NIST data in Fig. 5 to show the accuracy of the equation. As expected, the enthalpy depends on pressure as well as temperature because the refueling pressure is much higher than the conditions for an ideal gas state. The specific internal energy values are plotted with NIST data in Fig. 6. As presented in Fig. 6, $u - u_0$ values are accurately reproduced by Eq. (1). The internal energy is not as dependent on pressure as the enthalpy, but also changes with pressure due to a broad pressure range.

The temperature of hydrogen stored in an on-board tank increases from an ambient temperature up to 358.15 K while pressurizing from an initial pressure to NWP. Hydrogen

Fig. 5 Comparison of calculated specific enthalpy with NIST data

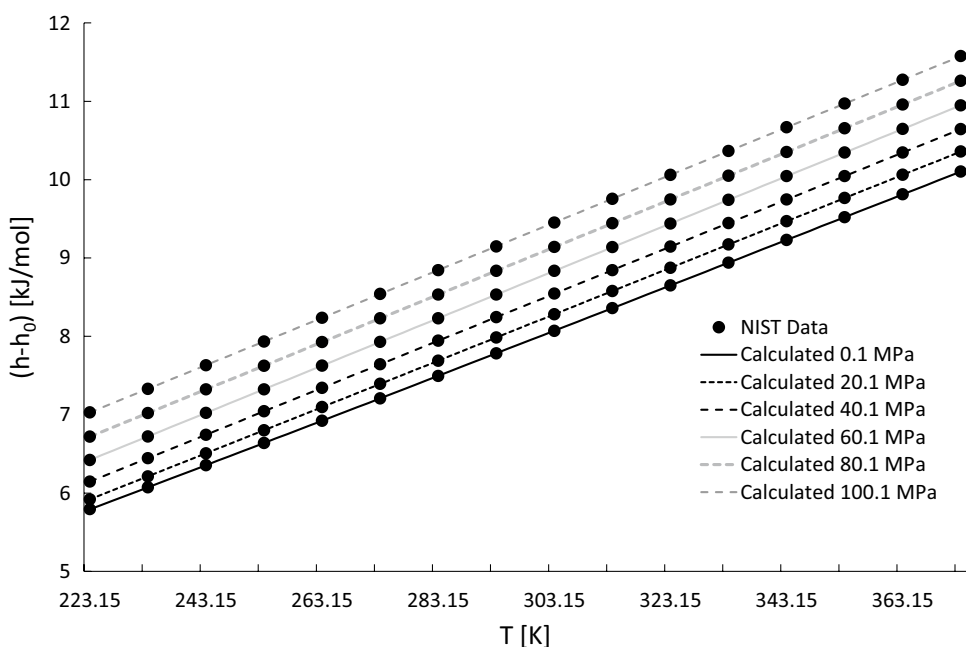
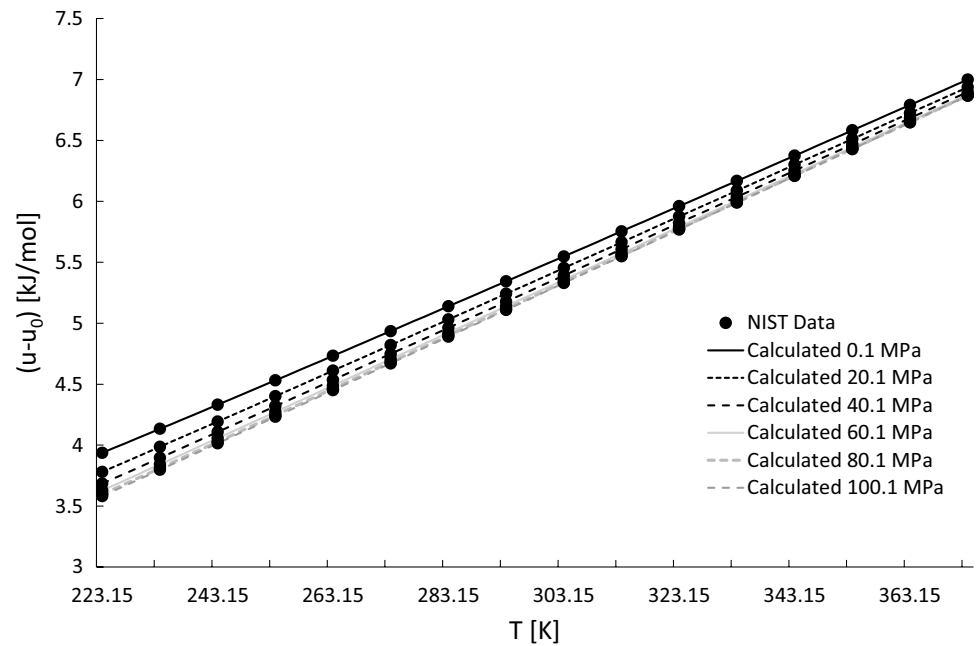


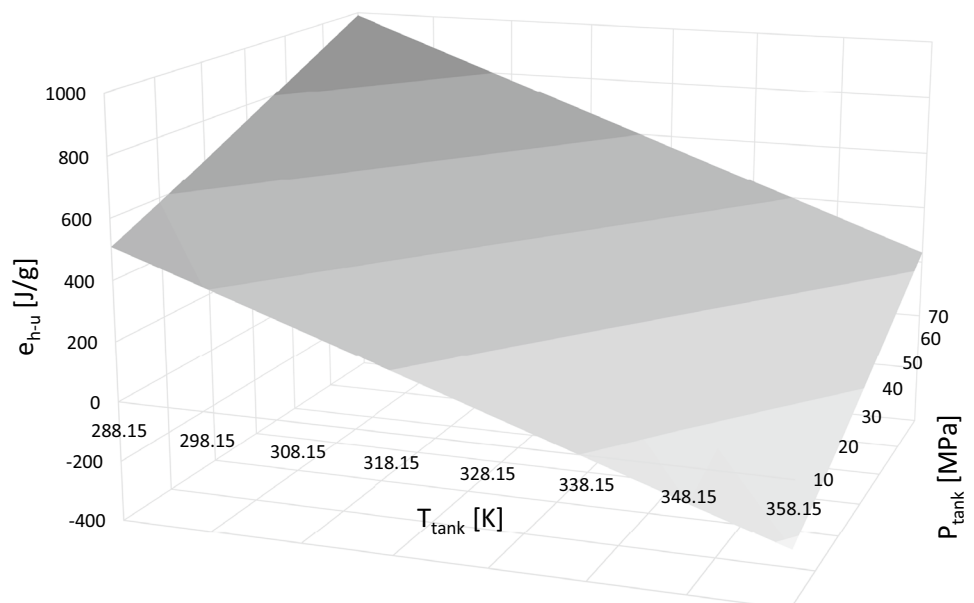
Fig. 6 Comparison of calculated specific internal energy with NIST data



flow entering an on-board tank is cooled down as low as to 233.15 K depending on HRS capability (see Fig. 1). The pressure of the inflow is controlled to be higher than the on-board tank pressure throughout a refueling process to secure desired mass flow rate. For a quantitative analysis, it is assumed to be 10 MPa higher than the on-board tank pressure. The energy difference defined by Eq. (7) is calculated with respect to tank pressure and temperature as presented in Fig. 7. The positive values mean an increase for the specific internal energy of hydrogen in the on-board tank due to the inlet flow, while the negative values which appear under high temperature and low pressure conditions indicate a decrease

for the specific internal energy by inflow. The temperature of the tank (T_{tank}) does not affect the enthalpy of hydrogen inflow, $(h - h_0)_{\text{in}}$, and only affects the internal energy of the hydrogen stored in the tank, $(u - u_0)_{\text{tank}}$, since the temperature entering the tank is fixed at 233.15 K, which is the hydrogen refueling temperature. The pressure flowing into the tank was set to be 10 MPa higher than the pressure of hydrogen in the tank. As shown in Figs. 5 and 6, the effect of pressure has a greater effect on the change in enthalpy than on the change in internal energy and, thus, the extent of the increase in enthalpy is larger than the increase in internal energy when the pressure increases. Due to these effects

Fig. 7 Energy differenced defined by Eq. (7) with respect to hydrogen temperature and pressure in tank



of temperature and pressure, the value of e_{h-u} has a negative value when the temperature of hydrogen in the tank is high and the pressure is low. In general, specific enthalpy is greater than specific internal energy, so the specific internal energy of hydrogen stored in an on-board tank increases by an inlet flow over a wide temperature and pressure range even if the temperature of the inlet flow is lowered to 233.15 K. As a refueling proceeds, the hydrogen in the tank changes from low temperature and pressure to high temperature and pressure and, thus, the internal energy increases due to the inflow of hydrogen during the filling process.

The kinetic energy per mass solely depends on the linear velocity (v_{in}) of an inflow. Generally, mass flow rate is controlled during the hydrogen refueling process. The linear velocity can be obtained from the mass flow rate and the kinetic energy (e_{ke}) can be expressed as follows.

$$e_{ke} = \frac{1}{2} \left(\frac{4\dot{m}_{in}}{\pi \rho_{in} d_{in}^2} \right)^2 \tag{8}$$

Hydrogen enters through an injector inserted into an on-board tank and the diameter of the injector is denoted as d_{in} in Eq. (8). The density of hydrogen flowing into the hydrogen storage tank (ρ_{in}) depends on temperature and pressure, but the temperature is kept constant because it goes through a pre-cooler. Therefore, the density can be assumed to depend only on the pressure at an injector in the tank.

In the course of the refueling of light-duty hydrogen vehicles, the maximum mass flow rate is limited to 60 g/s but it is expected to increase for heavy-duty vehicles up to 90 or 120 g/s. For calculation purposes, the kinetic energies per

mass of hydrogen flowing in at 233.15 K through an injector with a 6 mm diameter [58] are calculated and shown in Fig. 8.

As shown in Eq. (8), the kinetic energy of flowing hydrogen is proportional to the square of the mass flow rate. As the pressure of incoming hydrogen increases, its density increases accordingly and the linear velocity decreases at a given mass flow rate, which is reflected in the decreasing behavior of kinetic energy with pressure in Fig. 8.

The energy accumulation per unit mass of hydrogen flowing into the on-board storage tank can be defined as e_{in}

$$e_{in} = |e_{h-u}| + |e_{ke}| \tag{9}$$

The percentage contribution of kinetic energy ($= 100e_{ke}/e_{in}$) is estimated with on-board tank pressure and temperature. As presented in Fig. 9, as the mass flow rate increases, the kinetic energy contribution also increases. Therefore, to develop a thermodynamic model applicable to high flow rates, it is not appropriate to ignore the kinetic energy term in the energy balance. When the temperature of the hydrogen stored in the tank is high, the internal energy is also large, so the difference with the enthalpy of the incoming hydrogen decreases, of which temperature is assumed to be kept at 233.15 K by a pre-cooler. Consequently, the kinetic energy contribution increases as the tank temperature increases. Generally, as pressure increases, the contribution of kinetic energy decreases, but in the high-temperature and low-pressure region, e_{h-u} shows a negative value (Fig. 7) and the kinetic energy fraction tends to increase with pressure (Fig. 9c).

Fig. 8 Kinetic energy of hydrogen with mass flow rate and inlet pressure

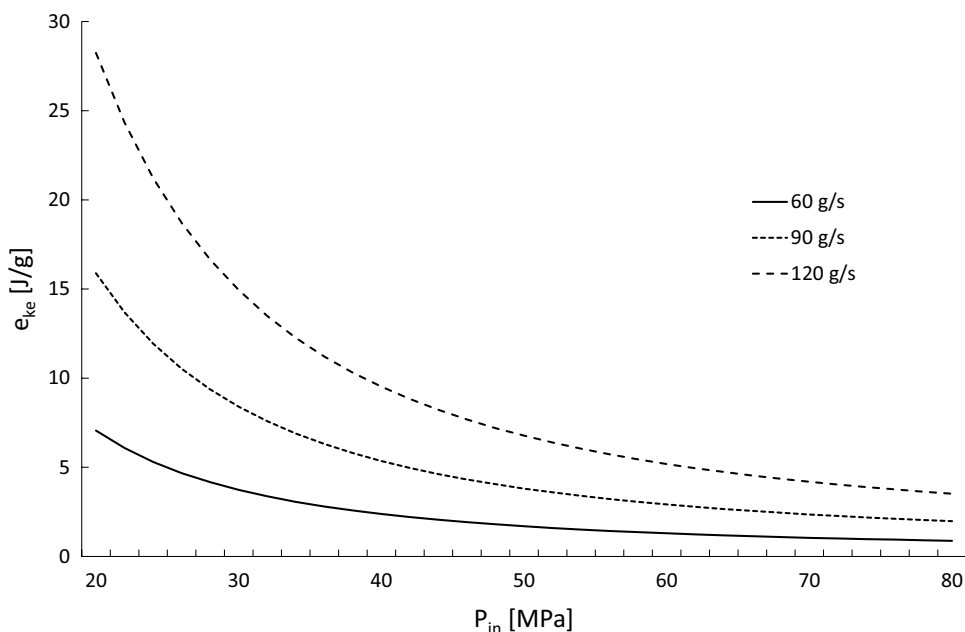
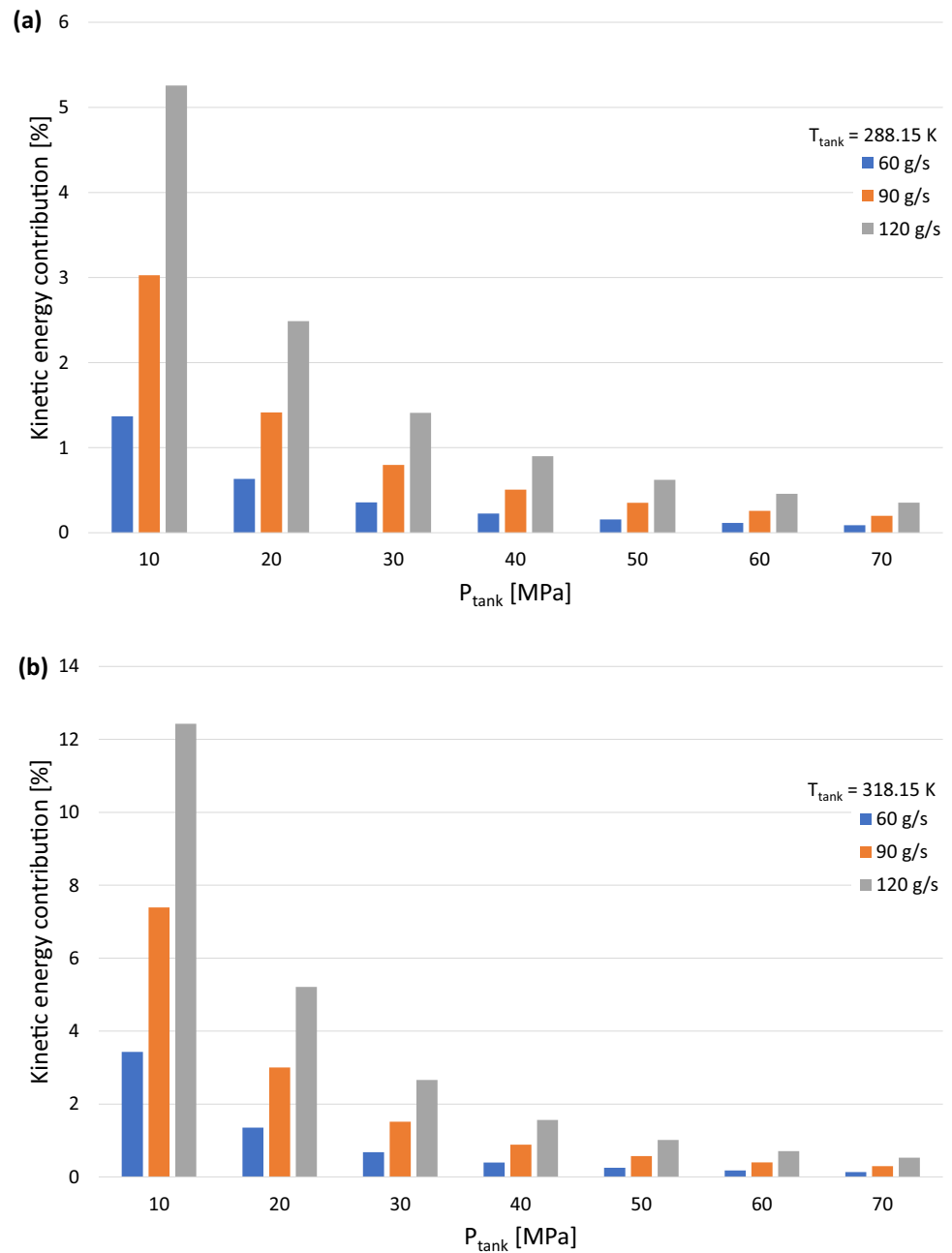


Fig. 9 Contribution of kinetic energy at hydrogen flowing into on-board tank with tank pressure and temperature



Stagnation Enthalpy

In thermodynamics and fluid mechanics, the concept of the stagnation enthalpy is usually applied to investigate a flow of compressible gases. The stagnation enthalpy of a fluid is the static enthalpy of the stream combined with the dynamic part from kinetic energy of the stream. It could be understood as the static enthalpy of the fluid at a stagnation point. Thermodynamic models describing the filling of hydrogen storage tanks can also use the stagnation enthalpy to set up an energy balance [59, 60]. However, thermodynamical caution must be taken with regard to heat capacity when using

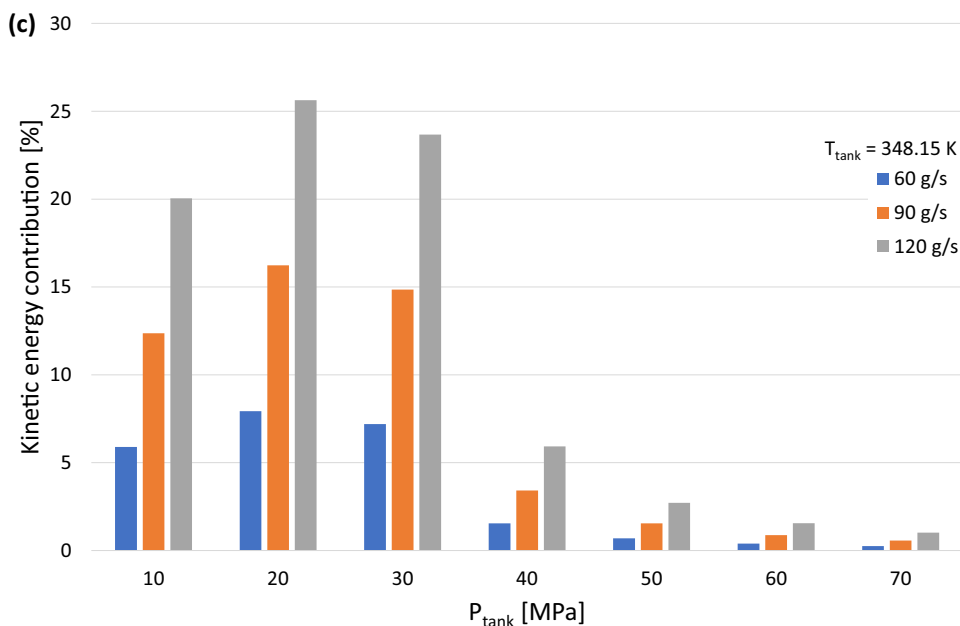
stagnation enthalpy to calculate the temperature of hydrogen in a tank.

The stagnation enthalpy at a tank inlet ($h_{\text{in},s}$) can be expressed in specific mass quantity as

$$h_{\text{in},s} = h_{\text{in}} + \frac{v_{\text{in}}^2}{2} \quad (10)$$

Enthalpy is directly related to heat capacity which measures the amount of heat required to change a substance's temperature. Unlike gases at ideal state, the heat capacity of a real gas at high pressure depends on pressure

Fig. 9 (continued)



as well as temperature. Using a following relationship between enthalpy and temperature, Eq. (10) can be rearranged to obtain stagnation inlet temperature ($T_{in,s}$),

$$h = h_0 + \int_{T_0}^T c_p dT = h_0 + \bar{c}_p(T - T_0) \tag{11}$$

$$T_{in,s} = T_{in} + \frac{v_{in}^2}{2\bar{c}_p} = T_{in} + \frac{1}{2\bar{c}_p} \left(\frac{4\dot{m}_{in}}{\pi \rho_{in} d_{in}^2} \right)^2 \tag{12}$$

Equation (12) is derived under an assumption of the same mean heat capacity (\bar{c}_p) up to $T_{in,s}$ and T_{in} , which can be formulated from Eq. (1).

$$\bar{c}_p = \frac{1}{T_{in} - T_0} \left[\sum_{i=0}^5 \sum_{j=0}^{5-i} \frac{a_{ij}}{i+1} T^{i+1} P^j \right]_{T_0}^{T_{in}} \tag{13}$$

During a hydrogen refueling process, \bar{c}_p of the hydrogen flowing into a tank at a given mass flow rate depends only on pressure since the inlet temperature of the hydrogen (T_{in}) is kept constant by a pre-cooler. Therefore, the stagnation inlet temperature denoted as $T_{in,s}$ also relies only on the inlet pressure and is always greater than T_{in} .

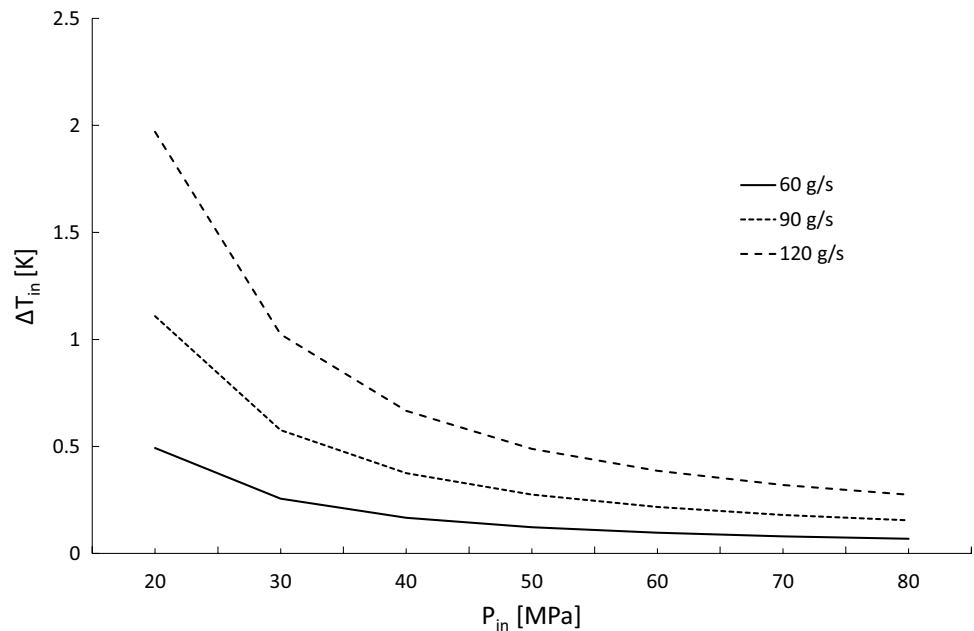
The temperature error which occurs when the stagnation enthalpy is used in the energy balance and the static temperature is applied instead of the stagnation temperature can be identified by calculating $\Delta T_{in}(=T_{in,s} - T_{in})$ from Eq. (12). At the lowest temperature at an inlet ($T_{in} = 233.15$ K), the temperature errors are delineated with a mass flow rate and pressure in Fig. 10.

Conclusions

It is possible to establish a safe method to fill hydrogen by understanding the phenomena that occur during a refueling process of highly compressed hydrogen into FCEVs. In addition to experimental studies, thermodynamic analysis including characteristics of hydrogen is necessary to develop safe hydrogen refueling procedures. Although various thermodynamic models have been proposed, the thermodynamic analysis of the hydrogen refueling process has not been systematically carried out and the feasibility of the models have not been verified. In this study, thermodynamic analysis results were presented based on an energy balance equation that describes the hydrogen refueling process by applying a generic correlation equation which accurately estimate hydrogen thermodynamic properties.

The Joule–Thomson (JT) effect, which explains the phenomenon of temperature change due to pressure change in an isenthalpic flow of fluids, is not directly related to the temperature increase of hydrogen stored in on-board tanks of FCEVs during refueling process. As can be recognized from the energy balance equation, the temperature rise of hydrogen in the on-board tank is determined by the amount of inflow energy, which depends on mass flow rate and specific enthalpy. The JT effect is observed under isenthalpic conditions, so even if the JT effect occurs at the inlet of the tank, there is no change in the enthalpy flowing in. From a thermodynamic perspective, the hydrogen refueling is a process in which enthalpy is converted into internal energy. Therefore, the JT effect may affect the local temperature distribution within the tank, but is not related to the overall temperature rise. The JT effect must be considered between

Fig. 10 Temperature differences between stagnation enthalpy and static enthalpy with mass flow rate



an upstream and a downstream of the pressure reducing valve. HRSs are usually operated in a cascade method or a buffer method. In the buffer method, where there is a large pressure difference at the beginning of hydrogen filling, a temperature rise of more than 35 K is expected after the pressure reducing valve, and in the cascade method with multi-stage storage tanks, a temperature rise of more than 20 K is expected when on-board tanks are connected with a high-pressure storage tank.

Kinetic energy is often ignored in the energy balance equation of thermodynamic models. In order to analyze the contribution of the kinetic energy, the effect of flow rate must be quantitatively compared based on the difference between the internal energy of stored hydrogen and the enthalpy of inflowing hydrogen. When the pressure in the tank is low, the kinetic energy effect is large due to the low internal energy of the stored hydrogen. As for high flow conditions such as 120 g/s, the kinetic energy contribution becomes greater and cannot be ignored to accurately estimate the temperature of stored hydrogen. Therefore, to develop a thermodynamic model applicable to various conditions, it is desirable not to ignore the kinetic energy term in the energy balance equation.

In some studies, stagnation enthalpy is used instead of static enthalpy. Such a case accurate results can be obtained only when the temperature is set to higher than temperature for the static enthalpy since the stagnation enthalpy includes a kinetic energy term.

Hydrogen refueling protocols for FCEVs which control the hydrogen filling process are difficult to develop only by experimental investigations and must be supported by simulation studies based on thermodynamic models. The results

of this study are expected to provide the fundamentals for a thermodynamic model for a large-capacity and high-speed hydrogen refueling protocol which is expected to be developed for heavy duty FCEVs. The thermodynamic analysis provided by the present work would be associated with a heat transfer model through on-board tank walls to develop a numerical model for the hydrogen refueling process. The numerical model would be used to analyze the temperature increase of hydrogen in the tank and propose a proper refueling method to secure safety on the process.

Acknowledgements This research was supported by the Korea Institute of Energy Technology Evaluation and Planning (KETEP) and the Ministry of Trade, Industry & Energy (MOTIE) of the Republic of Korea (Project No. 20203010040010). It was also supported by the Korea Agency for Infrastructure Technology Advancement (KAIA) and the Ministry of Land, Infrastructure and Transport (MOLIT) (Project No. 21OHTI-C163280-01).

Funding This article is funded by Korea Institute of Energy Technology Evaluation and Planning, 20203010040010, Byung Heung Park, Korea Agency for Infrastructure Technology Advancement, 21OHTI-C163280-01, Byung Heung Park.

References

1. M. Höök, X. Tang, *Energy Policy* **52**, 797 (2013)
2. N.Z. Muradov, T.N. Veziroğlu, *Int. J. Hydrogen Energy* **33**, 6804 (2008)
3. S. Dunn, *Int. J. Hydrogen Energy* **27**, 235 (2002)
4. C.C. Elam, C.E.G. Padró, G. Sandrock, A. Luzzi, P. Lindblad, E.F. Hagen, *Int. J. Hydrogen Energy* **28**, 601 (2003)
5. G. Marbán, T. Valdés-Solis, *Int. J. Hydrogen Energy* **32**, 1625 (2007)

6. J. Blazquez, R. Fuentes, B. Manzano, *Energy Policy* **147**, 111807 (2020)
7. J. Tian, L. Yu, R. Xue, S. Zhuang, Y. Shan, *Appl. Energy* **307**, 118205 (2022)
8. A. Kovač, M. Paranos, D. Marciuš, *Int. J. Hydrogen Energy* **46**, 10016 (2021)
9. A. Arcos-Vargas, *The role of the electric vehicle in the energy transition: a multidimensional approach* (Springer Nature, Berlin, 2020)
10. A. Dall-Orsoletta, P. Ferreira, G.G. Dranka, *Energy Convers. Manag.: X* **16**, 100271 (2022)
11. D. Wickham, A. Hawkes, F. Jalil-Vega, *Appl. Energy* **305**, 117740 (2022)
12. M. Muthukumar, N. Rengarajan, B. Velliyangiri, M. Omprakas, C. Rohit, U.K. Raja, *Mater. Today: Proc.* **45**, 1181 (2021)
13. A. Pramuanjaroenkij, S. Kakaç, *Int. J. Hydrogen Energy* **48**, 9401 (2023)
14. M. Ball, M. Weeda, *Int. J. Hydrogen Energy* **40**, 7903 (2015)
15. S. Singh, S. Jain, P. Venkateswaran, A.K. Tiwari, M.R. Nouni, J.K. Pandey, S. Goel, *Renew. Sustain. Energy Rev.* **51**, 623 (2015)
16. R. Gupta, M. F. Jalil, "An overview of using hydrogen in transportation sector as fuel", *Renewable Power for Sustainable Growth: Proceedings of International Conference on Renewal Power (ICRP 2020)*, (Springer, 2021), pp. 509–517
17. T. Stangarone, *Clean Technol. Environ. Policy* **23**, 509 (2021)
18. J.-H. Lee, J. Woo, *Sustainability* **12**, 10191 (2020)
19. J.-E. Shin, *Energies* **15**, 8983 (2022)
20. J. Alazemi, J. Andrews, *Renew. Sustain. Energy Rev.* **48**, 483 (2015)
21. X. Wang, J. Fu, Z. Liu, J. Liu, *Int. J. Hydrogen Energy* **48**, 1904 (2023)
22. SOA Engineers, *Fueling protocols for light duty gaseous hydrogen surface vehicles* (SAE International, Warrendale, 2016)
23. C.K. Chae, B.H. Park, Y.S. Huh, S.K. Kang, S.Y. Kang, H.N. Kim, *Int. J. Hydrogen Energy* **45**, 15390 (2020)
24. C.K. Chae, B.H. Park, S.K. Kang, J.-O. Choi, J.H. Park, W. Won, Y. Kim, *Korean J. Chem. Eng.* **39**, 2916 (2022)
25. T. Bourgeois, F. Ammouri, D. Baraldi, P. Moretto, *Int. J. Hydrogen Energy* **43**, 2268 (2018)
26. R. Caponi, A.M. Ferrario, E. Bocci, G. Valenti, M.D. Pietra, *Int. J. Hydrogen Energy* **46**, 18630 (2021)
27. E. Rothuizen, W. Mérida, M. Rokni, M. Wistoft-Ibsen, *Int. J. Hydrogen Energy* **38**, 4221 (2013)
28. M.-S. Kim, H.-K. Jeon, K.-W. Lee, J.-H. Ryu, S.-W. Choi, *Appl. Sci.* **12**, 4856 (2022)
29. H. Li, Z. Lyu, Y. Liu, M. Han, H. Li, *Int. J. Hydrogen Energy* **46**, 10396 (2021)
30. V. Ramasamy, E. Richardson, *Int. J. Heat Mass Transf.* **160**, 120179 (2020)
31. J. Liu, S. Zheng, Z. Zhang, J. Zheng, Y. Zhao, *Int. J. Hydrogen Energy* **45**, 9241 (2020)
32. Y. Wang, C. Decès-Petit, *Int. J. Hydrogen Energy* **45**, 32743 (2020)
33. J. Xiao, C. Bi, P. Bénard, R. Chahine, Y. Zong, M. Luo, T. Yang, *Int. J. Hydrogen Energy* **46**, 2936 (2021)
34. H. Tun, K. Reddi, A. Elgowainy, S. Poudel, *Int. J. Hydrogen Energy* **48**, 28869 (2023)
35. B.H. Park, D.H. Lee, *Korean J. Chem. Eng.* **39**, 902 (2022)
36. T. Kuroki, K. Nagasawa, M. Peters, D. Leighton, J. Kurtz, N. Sakoda, M. Monde, Y. Takata, *Int. J. Hydrogen Energy* **46**, 22004 (2021)
37. Y. Kang, S.M. Cho, D.K. Kim, *Int. J. Hydrogen Energy* **46**, 9174 (2021)
38. J.C. Yang, *Int. J. Hydrogen Energy* **34**, 6712 (2009)
39. C.N. Ranong, S. Maus, J. Hapke, G. Fieg, D. Wenger, *Heat Transfer Eng.* **32**, 127 (2011)
40. F. Olmos, V.I. Manousiouthakis, *Int. J. Hydrogen Energy* **38**, 3401 (2013)
41. E. Ruffio, D. Saury, D. Petit, *Int. J. Hydrogen Energy* **39**, 12701 (2014)
42. Y.-L. Liu, Y.-Z. Zhao, L. Zhao, X. Li, H.-G. Chen, L.-F. Zhang, H. Zhao, R.-H. Sheng, T. Xie, D.-H. Hu, *Int. J. Hydrogen Energy* **35**, 2627 (2010)
43. C. Dicken, W. Merida, *J. Power. Sources* **165**, 324 (2007)
44. M. Monde, Y. Mitsutake, P. L. Woodfield, S. Maruyama, *Heat Transfer—Asian Research: Co-sponsored by the Society of Chemical Engineers of Japan and the Heat Transfer Division of ASME*, **36**, 13 (2007)
45. T. Johnson, R. Bozinoski, J. Ye, G. Sartor, J. Zheng, J. Yang, *Int. J. Hydrogen Energy* **40**, 9803 (2015)
46. M. Deymi-Dashtebayaz, M. Farzaneh-Gord, N. Nooralipoor, H. Niazmand, *Braz. J. Chem. Eng.* **33**, 391 (2016)
47. H. Luo, J. Xiao, P. Bénard, R. Chahine, T. Yang, *Int. J. Hydrogen Energy* **51**, 664 (2024)
48. K. Reddi, A. Elgowainy, E. Sutherland, *Int. J. Hydrogen Energy* **39**, 19169 (2014)
49. L. Viktorsson, J.T. Heinonen, J.B. Skulason, R. Unnthorsson, *Energies* **10**, 763 (2017)
50. E. Talpacci, M. Reuß, T. Grube, P. Cilibrizzi, R. Gunnella, M. Robinus, D. Stolten, *Int. J. Hydrogen Energy* **43**, 6256 (2018)
51. Y. Yu, C. Lu, S. Ye, Z. Hua, C. Gu, *Int. J. Hydrogen Energy* **47**, 13430 (2022)
52. Z. Tian, H. Lv, W. Zhou, C. Zhang, P. He, *Int. J. Hydrogen Energy* **47**, 3033 (2022)
53. B.H. Park, C.K. Chae, *Int. J. Hydrogen Energy* **47**, 4185 (2022)
54. P.J. Linstrom, W.G. Mallard, *J. Chem. Eng. Data* **46**, 1059 (2001)
55. J.-Q. Li, Y. Chen, Y.B. Ma, J.-T. Kwon, H. Xu, J.-C. Li, *Case Stud. Therm. Eng.* **41**, 102678 (2023)
56. E. Rothuizen, M. Rokni, *Int. J. Hydrogen Energy* **39**, 582 (2014)
57. M. Monde, P. Woodfield, T. Takano, M. Kosaka, *Int. J. Hydrogen Energy* **37**, 5723 (2012)
58. N. De Miguel, B. Acosta, P. Moretto, R.O. Cebolla, *Int. J. Hydrogen Energy* **41**, 19447 (2016)
59. M. Farzaneh-Gord, M. Deymi-Dashtebayaz, H.R. Rahbari, H. Niazmand, *Int. J. Hydrogen Energy* **37**, 3500 (2012)
60. E. Rothuizen, B. Elmegaard, M. Rokni, *Int. J. Hydrogen Energy* **45**, 9025 (2020)

Publisher's Note Springer Nature remains neutral with regard to jurisdictional claims in published maps and institutional affiliations.

Springer Nature or its licensor (e.g. a society or other partner) holds exclusive rights to this article under a publishing agreement with the author(s) or other rightsholder(s); author self-archiving of the accepted manuscript version of this article is solely governed by the terms of such publishing agreement and applicable law.